ACTA CHEMICA SCANDINAVICA 13 (1959) 1193–1208

An X-Ray Investigation of the Nickel-Boron System

The Crystal Structures of Orthorhombic and Monoclinic Ni_4B_3

STIG RUNDQVIST

Institute of Chemistry, University of Uppsala, Uppsala, Sweden

The Ni-B system has been investigated with X-ray powder and single-crystal methods in the range Ni_3B-NiB. In addition to the previously known intermediate phases, Ni_3B, Ni_2B and NiB, the existence of two other phases, both with the ideal compositions Ni_4B_3 but one orthorhombic and the other monoclinic, has been established. The following two-phase regions have been found: Ni_3B + Ni_2B, Ni_2B + orthorhombic Ni_4B_3, orthorhombic Ni_4B_3 + monoclinic Ni_4B_3 and monoclinic Ni_4B_3 + NiB. The unit cell of orthorhombic Ni_4B_3 varies slightly with composition: the dimensions in two-phase Ni_2B + orthorhombic Ni_4B_3 alloys are the following: $a = 11.953$ Å, $b = 2.981$ Å, $c = 6.569$ Å and in two-phase orthorhombic Ni_4B_3 + monoclinic Ni_4B_3 alloys: $a = 11.973$ Å, $b = 2.985$ Å, $c = 6.584$ Å. The unit cell dimensions of monoclinic Ni_4B_3 are $a = 6.430$ Å, $b = 4.882$ Å, $c = 7.818$ Å, $\beta = 103°18'$. No unit cell variation of the latter phase has been found.

The crystal structures of the two new phases have been determined and refined from single-crystal intensity data. The space group of orthorhombic Ni_4B_3 is $P\,n\,m\,a$; the unit cell contains sixteen nickel atoms and twelve boron atoms situated in 4(*c*) positions. Two-thirds of the boron atoms form infinite zig-zag chains, while one-third have no close boron contacts. There are probably boron vacancies in the structure.

The space group of monoclinic Ni_4B_3 is $C\,2/c$. Sixteen nickel atoms are situated in two 8(*f*) positions, eight boron atoms in one 8(*f*) position and four boron atoms in one 4(*e*) position. All boron atoms are connected in infinite chains.

Among the borides of the iron group metals, the nickel borides have received comparatively little attention. The nickel-boron equilibrium diagram has not been accurately determined, but it appears that the Ni-B system is much more complex than either the Fe-B or the Co-B systems. A short summary of the previous work on the nickel borides is given below.

Giebelshausen [1] made a thermal and microscopic analysis in the range 0—60 atom-% boron and claimed the existence of the phases Ni_2B, Ni_3B_2, NiB and Ni_2B_3. Recently, Hoppin III [2] made a microscopic and thermal ana-

lysis in the range 0—17 atom-% boron and found a maximum solid solubility of boron in nickel of 3.7 atom-% at 1 082°C. Bjurström [3] studied the Ni-B system with X-ray powder methods and determined the crystal structure of Ni_2B to be that of the $CuAl_2$ (C 16) type. A phase analysis with X-ray powder methods by Andersson and Kiessling [4] showed the existence of at least four intermediate phases with compositions close to Ni_3B, Ni_2B, Ni_3B_2 and NiB. The crystal structure of NiB was determined by Blum [5] who found NiB to be isostructural with CrB [6]. The preparation of nickel borides by igneous electrolysis was studied by Marion [7], who prepared in addition to Ni_2B and NiB, two phases with compositions between 33 1/3 and 50 atom-% boron and one phase with a boron content larger than 50 atom-%.

At this Institute, the Ni-B system has been reinvestigated with X-ray powder and single-crystal methods, and in previous papers [8,9] the cementite type structure of Ni_3B has been reported. The structure of Ni_3B has been confirmed by Fruchart and Michel [10], and some physical and chemical properties of Ni_3B have been studied by Blok, Kozlova, Lashko and Shpunt [11], who also published X-ray powder data of Ni_3B. Their powder data are in agreement with the present author's findings [8,9].

EXPERIMENTAL

The samples were prepared by heating nickel powder (99.9 %, kindly donated by Mond Nickel Co., Ltd) and boron powder (99.7 % or better, kindly donated by Borax Consolidated Ltd) in evacuated, sealed silica tubes at temperatures between 750° and 950°C. It has been found that the silica tubes are attacked by Ni-B mixtures at elevated temperatures which results mainly in the formation of a ternary compound with the ideal composition Ni_6Si_3B [12]. Because of this the samples were protected from direct contact with the silica by placing them in small Al_2O_3 crucibles inside the silica tubes. No appreciable reaction between Al_2O_3 and the nickel borides was observed. However, the compositions of boron-rich alloys did not correspond to the weighed amounts of the starting materials, since varying amounts of boron were unavoidably lost during the reactions. It was, therefore, often necessary to make a large number of samples in order to obtain an alloy with a composition within a desired narrow range.

X-Ray powder photographs were taken with Guinier-type focusing cameras with Cu$K\alpha$ and Cr$K\alpha$ radiations. Each powder film was calibrated with CaF_2 as internal standard ($\lambda_{CuK\alpha} = 1.5418$ Å, $\lambda_{CrK\alpha} = 2.2909$ Å, CaF_2: $a = 5.4630$ Å). The accuracy of the lattice parameters given in this paper is greater than 0.05 %.

For the structure determinations, Weissenberg photographs were taken with MoK radiation of small single-crystal fragments selected from the crushed alloys. The multiple-film technique was used with thin iron foils between successive films, and the intensities were estimated visually by comparison with a standard intensity scale. No correction for absorption or anomalous scattering was applied. Fourier summations were made with the Hägg-Laurent machine and with Beevers-Lipson strips. Atomic scattering factors were interpolated from tables given by Thomas and Umeda [13] for nickel and by Ibers [14] for boron.

THE PHASE ANALYSIS

Since the main purpose of the present investigation was to study the crystal structures of the intermediate phases, the phase analysis was performed with X-ray powder methods only.

The existence of the previously reported phases Ni_3B, Ni_2B and NiB was confirmed. The unit cell dimensions were determined (see Table 1) and were

in agreement with the results of earlier measurements. No nickel boride with the composition Ni_3B_2, as reported by Giebelshausen [1], was found. Instead, the existence of two new phases, both with compositions near Ni_4B_3, was established. This is in agreement with the findings of Marion [7], who reported two phases of composition within the range Ni_2B-NiB. The X-ray measurements showed that the owo phases possessed orthorhombic and monoclinic symmetry, respectively, and the phases are therefore denoted in the following text as *o*-Ni_4B_3 and *m*-Ni_4B_3.

Since *o*-Ni_4B_3 and *m*-Ni_4B_3 appeared to have the same composition, the existence of a polymorphic transition was suspected. Samples of *o*-Ni_4B_3 and *m*-Ni_4B_3, the powder photographs of which were free from traces of Ni_2B or NiB, were subjected to various heat treatments and rapid quenchings, but no signs of transitions in the solid state were observed. For *m*-Ni_4B_3, no lattice parameter variations were found; but for *o*-Ni_4B_3, a small decrease of the unit cell was indicated in alloys quenched from higher temperatures.

The two-phase regions Ni_3B + Ni_2B, Ni_2B + *o*-Ni_4B_3 and *m*-Ni_4B_3 + NiB were found in the temperature range 750°—950°C, but no two-phase regions *o*-Ni_4B_3 + NiB or Ni_2B + *m*-Ni_4B_3 were observed. Attempts to prepare two-phase *o*-Ni_4B_3 + *m*-Ni_4B_3 alloys were successful in only a few cases. One alloy was heated for 14 days at 850°C, and the two phases still coexisted after the heat treatment. The lattice parameters of *o*-Ni_4B_3 were slightly larger in two-phase *o*-Ni_4B_3 + *m*-Ni_4B_3 alloys than in Ni_2B + *o*-Ni_4B_3 alloys (see Table 1); this indicates that the unit cell of *o*-Ni_4B_3 increases with increasing B/Ni ratio.

From the single-crystal structure determinations (*vide infra*) it was evident that the ideal composition of both *o*-Ni_4B_3 and *m*-Ni_4B_3 should be Ni_4B_3. A study of the available space in the structures showed that the lattices could hardly accommodate more boron or nickel atoms than the stoichiometrical number. Any deviation from stoichiometry must therefore be due either to the existence of lattice vacancies or to boron-nickel substitution.

It is quite clear that additional information, *e.g.*, from microscopic and thermal analytical investigations, must be available before any definite conclusions can be drawn about the phase relationships in the nickel-boron system. However, the following interpretation is suggested by the present observations.

Around the composition 40—43 atom-% boron, two discrete intermediate phases, *o*-Ni_4B_3 and *m*-Ni_4B_3, exist at least in the temperature range 750°—950°C. The two-phase range is probably very narrow, as indicated by the diffi-

Table 1. Crystallographic data of the nickel borides (unit cell edges in Å).

Boride	Structure type	Space group	*a*	*b*	*c*	*β*
Ni_3B	*D* O_{11}	*Pnma*	5.211	6.619	4.389	—
Ni_2B	*C* 16	*I4/mcm*	4.989	—	4.246	—
o-Ni_4B_3 (metal-rich)		*Pnma*	11.953	2.981	6.569	—
o-Ni_4B_3 (boron-rich)		*Pnma*	11.973	2.985	6.584	—
m-Ni_4B_3		*C2/c*	6.430	4.882	7.818	103°18′
NiB	CrB	*Cmcm*	2.928	7.391	2.964	—

Table 2. Powder data for metal-rich orthorhombic Ni_4B_3 (Cr*Ka* radiation).

h k l	$\sin^2\Theta_o \times 10^4$	$\sin^2\Theta_c \times 10^4$	I_o	I_c	*hkl*	$\sin^2\Theta_o \times 10^4$	$\sin^2\Theta_c \times 10^4$	I_o	I_c
200	368	367	v.w	10	410	2 944	2 945	st	484
101	—	396	—	0	212	3 059	3 060	v.st	714
201	672	671	v.w	3	203	3 104	3 104	v.w	9
301	—	1 131	—	0	411	3 248	3 249	m	145
002	1 217	1 216	v.w	12	600	3 305	3 306	w	19
102	1 308	1 308	w	26	502	} 3 517	3 512	} st	18
400	1 470	1 469	m	72	312		3 519		353
202	1 585	1 584	m	117	303	3 564	3 563	st	364
401	1 774	1 773	v.w	7	601	3 609	3 610	st	489
011	1 781	1 780	w	29	511	4 075	4 076	st	385
210	—	1 843	—	0	412	4 164	4 162	w	27
111	1 872	1 872	w	33	403	} 4 212	4 206	} st	211
302	2 041	2 043	m	110	013		4 213		244
211	2 147	2 147	st	295	113	4 307	4 305	m	107
501	} 2 606	2 600	} st	12	602	4 524	4 522	m	131
311		2 607		199	213	4 583	4 581	w	26
402	2 684	2 686	w	26	610	—	4 782	—	9
112	2 784	2 784	m	150	701	4 803	4 804	m	139
103	2 828	2 829	m	170					

culties of obtaining a two-phase *o*-Ni_4B_3 + *m*-Ni_4B_3 alloy (compare the experimental part of the paper). The monoclinic phase is believed to correspond closely to the stoichiometrical composition and may be assigned the formula Ni_4B_3. The crystal lattice of the orthorhombic phase probably contains a varying amount of boron vacancies, which are never completely filled. The formula of this phase may therefore be written Ni_4B_{3-x}, $x > 0$. The number of vacancies probably increases with increasing temperature.

Table 3. Powder data for monoclinic Ni_4B_3 (Cr*Ka* radiation).

hkl	$\sin^2\Theta_o \times 10^4$	$\sin^2\Theta_c \times 10^4$	I_o	I_c	*hkl*	$\sin^2\Theta_o \times 10^4$	$\sin^2\Theta_c \times 10^4$	I_o	I_c
110	886	886	w	49	$\bar{3}11$	3 412	3 414	st	431
002	907	907	v.w	11	$\bar{2}21$	3 515	3 516	w	89
$\bar{1}11$	—	985	—	2	220	3 543	3 543	v.st	684
111	1 240	1 240	w	38	310	3 567	3 567	m	177
200	—	1 340	—	1	004	3 625	3 626	st	385
$\bar{1}12$	1 539	1 538	m	171	$\bar{3}12$	3 713	3 713	m	246
$\bar{2}02$	1 739	1 740	st	319	$\bar{2}22$	3 942	3 942	w	87
112	2 047	2 046	v.w	10	$\bar{2}04$	3 952	3 953	w	68
020	2 202	2 202	v.w	12	$\bar{1}14$	4 005	4 005	m	221
021	2 431	2 429	m	160	221	4 023	4 023	m	171
$\bar{1}13$	2 544	2 546	st	298	311	4 177	4 174	w	74
202	2 753	2 754	v.st	579	023	4 244	4 242	w	121
022	3 108	3 109	v.st	737	$\bar{3}13$	4 467	4 466	w	99
113	—	3 306	—	3	$\bar{2}23$	4 823	4 822	w	36

Unit cell dimensions of the nickel borides are given in Table 1. For identification purposes, powder data for o-Ni_4B_3 and m-Ni_4B_3 are given in Tables 2 and 3. It may be noted that for o-Ni_4B_3, the ratio a/b is nearly equal to 4; this makes it somewhat difficult to index correctly the powder lines without knowledge of the intensities of the reflexions.

THE CRYSTAL STRUCTURE DETERMINATION OF ORTHORHOMBIC Ni_4B_3

It is evident from the foregoing text that a knowledge of the crystal structures of o-Ni_4B_3 and m-Ni_4B_3 is valuable from the phase-analytical point of view. Furthermore, the structures also seemed interesting for crystal-chemical reasons, and complete single-crystal structure determinations of both phases were therefore made.

From the measured density value, 7.4 g. cm^{-3} the unit cell content of o-Ni_4B_3 was calculated to be 16 nickel atoms and 12 boron atoms, the unit cell volume being 234—235 Å^3. The following conditions which limit possible reflexions were found: (h k 0) for $h = 2n$, (0 k l) for $k + l = 2n$. The two space groups $Pn2_1a$ and $Pnma$ where therefore possible. Since the b-axis was only 2.98 Å, the 8(d) position of nickel atoms in space group $Pnma$ was ruled out. A study of the intensity material from the layer lines 0—3 around the b axis showed that the corresponding (h 0 l) and (h 2 l) intensities were equal (apart from the normal decline), and the same was true for the (h 1 l) and (h 3 l) reflexions. The simplest interpretation of these facts was to assume that the space group is $Pnma$ with all nickel atoms (and possibly also the boron atoms) in 4(c) positions. The Patterson section $P(x\ 0\ z)$ was computed with the three-dimensional intensity material. The heights and positions of the maxima were in accordance with the above assumptions. Rough parameter values were obtained for the four sets of nickel atoms, and signs were calculated for the $F(h\ 0\ l)$ values. The electron density projection $\varrho\ (x\ z)$ was then calculated and, in addition to the expected nickel maxima, faint boron maxima corresponding to three 4(c) positions were discernible. The x and z parameters of the atoms were refined with successive difference syntheses. The final difference synthesis map, in which all nickel atoms were subtracted, showed well resolved boron maxima. The heights of the B_{II} and B_{III} maxima were almost equal, whereas the B_I maximum was lower and not symmetrical in shape. As measured on this map, the position of the B_I maximum corresponded to the parameters $x = 0.469$, $z = 0.428$, and resulted in a rather uneven distribution of Ni—B_I distances. The parameter values $x = 0.473$, $z = 0.430$ gave a more reasonable environment for the B_I atoms. Since this shift was permissible with regard to the accuracy of the experimental intensity material, these parameters were considered to be more reliable than those obtained directly from the electron density map. The difference in height between the B_I and the B_{II} and B_{III} maxima points to the possible existence of boron vacancies in the structure, but the experimental intensity data do not permit drawing any significant conclusion. After the last refinement, the R value 0.085 was obtained for the 117 observed $|F(h\ 0\ l)|$-values, when an empirical temperature factor with $B = 0.39$ Å^2 was applied. Observed and calculated $F(h\ 0\ l)$-values are given in Table 4.

Table 4. Observed and calculated $F(h0l)$-values for orthorhombic Ni_4B_3.

h 0 l	F_o	F_c	h 0 l	F_o	F_c
0 0 0	—	508	19 0 2	51.8	−52.2
2 0 0	21.3	−14.3	20 0 2	—	12.3
4 0 0	79.6	−82.2	21 0 2	29.3	35.1
6 0 0	61.9	53.5	1 0 3	101.6	113.4
8 0 0	—	−13.8	2 0 3	26.4	26.0
10 0 0	65.1	61.2	3 0 3	133.3	−163.5
12 0 0	121.0	−121.0	4 0 3	103.6	114.9
14 0 0	—	20.2	5 0 3	—	−13.0
16 0 0	—	25.5	6 0 3	—	13.6
18 0 0	—	−14.8	7 0 3	70.7	70.2
20 0 0	54.8	49.5	8 0 3	70.5	70.7
22 0 0	—	−5.3	9 0 3	28.7	20.5
24 0 0	—	12.3	10 0 3	—	4.3
26 0 0	—	19.3	11 0 3	45.9	−41.1
28 0 0	38.4	−29.8	12 0 3	52.7	−51.7
1 0 1	—	− 0.2	13 0 3	—	−19.3
2 0 1	—	− 8.2	14 0 3	—	− 2.7
3 0 1	—	− 3.7	15 0 3	62.7	57.6
4 0 1	26.0	−19.6	16 0 3	50.4	−50.2
5 0 1	34.6	−29.1	17 0 3	—	−23.4
6 0 1	149.5	−189.7	18 0 3	—	− 9.2
7 0 1	85.6	84.2	19 0 3	—	5.0
8 0 1	—	− 5.0	20 0 3	—	− 0.9
9 0 1	62.8	−60.9	0 0 4	41.8	36.2
10 0 1	50.9	47.0	1 0 4	69.3	69.4
11 0 1	28.2	−29.7	2 0 4	87.7	96.2
12 0 1	—	15.6	3 0 4	40.9	42.4
13 0 1	88.5	86.8	4 0 4	27.2	−20.3
14 0 1	27.0	28.9	5 0 4	37.3	−39.0
15 0 1	34.7	−34.9	6 0 4	—	10.6
16 0 1	—	11.7	7 0 4	27.9	−27.6
17 0 1	18.0	−25.7	8 0 4	—	− 9.2
18 0 1	56.2	50.2	9 0 4	47.3	45.8
19 0 1	—	11.8	10 0 4	135.1	−141.8
20 0 1	—	5.7	11 0 4	27.8	28.3
21 0 1	—	3.7	12 0 4	26.6	23.7
22 0 1	47.1	−45.0	13 0 4	—	−21.5
0 0 2	30.8	−30.9	14 0 4	—	9.3
1 0 2	32.2	33.0	15 0 4	—	−14.9
2 0 2	84.7	−76.6	16 0 4	43.0	−39.7
3 0 2	84.0	−82.8	17 0 4	—	14.5
4 0 2	49.7	−43.7	18 0 4	27.8	30.6
5 0 2	39.1	36.5	19 0 4	—	8.6
6 0 2	82.3	86.2	20 0 4	—	35.6
7 0 2	88.5	96.8	21 0 4	—	−10.9
8 0 2	38.2	33.8	22 0 4	33.7	33.2
9 0 2	80.8	−77.7	30 0 4	40.2	−33.2
10 0 2	—	− 3.0	1 0 5	20.4	15.0
11 0 2	16.6	16.2	2 0 5	46.1	−44.6
12 0 2	57.5	58.2	3 0 5	71.4	−77.2
13 0 2	—	− 2.7	4 0 5	87.4	−99.7
14 0 2	46.4	42.2	5 0 5	57.5	57.9
15 0 2	26.4	29.2	6 0 5	13.1	19.8
16 0 2	53.8	−59.4	7 0 5	—	− 3.9
17 0 2	—	0.9	8 0 5	31.4	−30.6
18 0 2	44.4	−45.5	9 0 5	23.1	−23.2

Table 4. Contd.

h 0 *l*	F_o	F_c	*h* 0 *l*	F_o	F_c
10 0 5	33.8	−30.8	3 0 9	27.9	−32.2
11 0 5	—	1.8	4 0 9	25.2	−29.0
12 0 5	—	21.8	5 0 9	49.2	−56.1
13 0 5	24.2	32.5	6 0 9	61.9	−62.7
14 0 5	48.3	50.0	7 0 9	69.3	70.1
15 0 5	—	21.3	8 0 9	—	0.1
16 0 5	58.3	54.1	9 0 9	—	2.6
17 0 5	49.8	−49.1	10 0 9	—	− 3.3
23 0 5	33.8	−35.4	11 0 9	24.3	−33.2
0 0 6	45.5	47.7	12 0 9	—	−11.0
1 0 6	35.9	−34.6	13 0 9	—	17.9
2 0 6	51.3	−56.6	14 0 9	41.7	43.2
3 0 6	42.4	41.0	0 0 10	—	−13.3
4 0 6	91.7	−100.4	1 0 10	66.4	65.8
5 0 6	—	17.7	2 0 10	40.0	−35.2
6 0 6	41.7	38.5	3 0 10	—	6.1
7 0 6	—	−13.4	4 0 10	—	−14.1
8 0 6	92.7	99.4	5 0 10	—	29.0
9 0 6	56.3	55.0	6 0 10	23.9	29.7
10 0 6	—	− 2.1	7 0 10	—	0.5
11 0 6	42.6	−42.2	8 0 10	—	13.2
12 0 6	—	4.6	9 0 10	—	5.6
13 0 6	—	14.4	10 0 10	—	8.0
1 0 7	—	− 5.8	11 0 10	—	25.7
2 0 7	98.3	102.0	1 0 11	—	11.3
3 0 7	—	− 8.2	2 0 11	—	− 6.2
4 0 7	—	− 1.6	3 0 11	—	−18.3
5 0 7	—	−16.6	4 0 11	28.5	30.0
6 0 7	—	16.5	5 0 11	—	24.6
7 0 7	46.5	39.4	6 0 11	—	10.0
8 0 7	—	16.8	7 0 11	—	− 3.5
9 0 7	23.7	−35.5	8 0 11	—	33.8
10 0 7	24.3	25.3	9 0 11	—	−15.1
11 0 7	—	−14.7	10 0 11	—	−20.5
12 0 7	—	−11.5	11 0 11	—	− 2.9
13 0 7	56.5	57.0	12 0 11	45.1	−41.4
14 0 7	74.7	−72.2	0 0 12	46.8	46.0
26 0 7	31.1	30.0	1 0 12	—	14.8
0 0 8	78.2	87.4	2 0 12	33.2	31.9
1 0 8	—	−17.6	3 0 12	—	1.4
2 0 8	—	− 7.5	4 0 12	21.0	−32.6
3 0 8	—	−11.7	5 0 12	—	−16.3
4 0 8	—	12.5	6 0 12	—	− 3.5
5 0 8	—	0.9	7 0 12	—	7.8
6 0 8	—	26.2	8 0 12	—	28.1
7 0 8	24.3	25.5	9 0 12	—	5.5
8 0 8	68.1	−65.5	10 0 12	52.2	−54.2
9 0 8	—	− 1.6	1 0 13	—	7.6
10 0 8	—	−26.5	2 0 13	—	1.8
11 0 8	—	−32.4	3 0 13	—	−19.8
12 0 8	23.6	−26.0	4 0 13	—	−24.7
13 0 8	—	11.5	5 0 13	—	23.9
20 0 8	72.0	65.2	6 0 13	30.2	−39.2
1 0 9	—	26.4	11 0 14	27.5	−30.7
2 0 9	—	−19.2			

The final structure of orthorhombic Ni_4B_3 is the following:

Space group $Pnma$—(D_{2h}^{16}), $Z = 4$

$a = 11.953$ Å, $b = 2.981$ Å, $c = 6.569$ Å, $U = 234.1$ Å^3.

(Unit cell dimensions were measured on powder photographs of the alloy, from which the actual single-crystal specimen was selected.)

All atoms in 4(*c*) positions:

	x	*z*
Ni_I	0.148_6	-0.009_7
Ni_{II}	0.449_8	0.751_1
Ni_{III}	0.199_7	0.378_0
Ni_{IV}	0.376_3	0.167_5
B_I	0.47_3	0.43_0
B_{II}	0.03_7	0.48_1
B_{III}	0.26_5	0.67_3

Interatomic distances are given in Table 5.

Table 5. Interatomic distances in orthorhombic Ni_4B_3 (Distances shorter than 3.0 Å listed).

	Ni_I	Ni_{II}	Ni_{III}	Ni_{IV}	B_I	B_{II}	B_{III}
Ni_I	2.98 (2)	2.56 (2) 2.86	2.46 (2) 2.63	2.76 (2) 2.97	2.1_2 (2) 2.1_7		2.1_8 (2) 2.5_1
Ni_{II}	2.56 (2) 2.86	2.98 (2)	2.48 (2)	2.62 (2) 2.88	2.1_2 (2) 2.1_3	2.0_5 (2) 2.1_3	2.2_7
Ni_{III}	2.46 (2) 2.63	2.48 (2)	2.98 (2)	2.53 2.64 (2)		2.0_6	2.0_6 (2) 2.0_9
Ni_{IV}	2.76 (2) 2.97	2.62 (2) 2.88	2.53 2.64 (2)	2.98 (2)	2.0_8	2.1_6 (2) 2.1_9	2.2_6 (2)
B_I	2.1_2 (2) 2.1_7	2.1_3 (2) 2.1_3		2.0_8	1.8_6 (2)		
B_{II}		2.0_5 (2) 2.1_3	2.0_6	2.1_6 (2) 2.1_9		1.7_5 (2)	
B_{III}	2.1_8 (2) 2.5_1	2.2_7	2.0_6 (2) 2.0_9	2.2_6 (2)			

DESCRIPTION OF THE ORTHORHOMBIC Ni_4B_3 STRUCTURE

A projection of the structure on the *ac*-plane is shown in Fig. 1. The nickel atom lattice can be described as built-up by interconnected trigonal prisms of nickel atoms. The boron atoms are situated in the centers of these prisms. The B_I and B_{II} atoms form two separate boron chains running zig-zag throughout the structure in the *b* direction, whereas the B_{III} atoms have no close boron contacts.

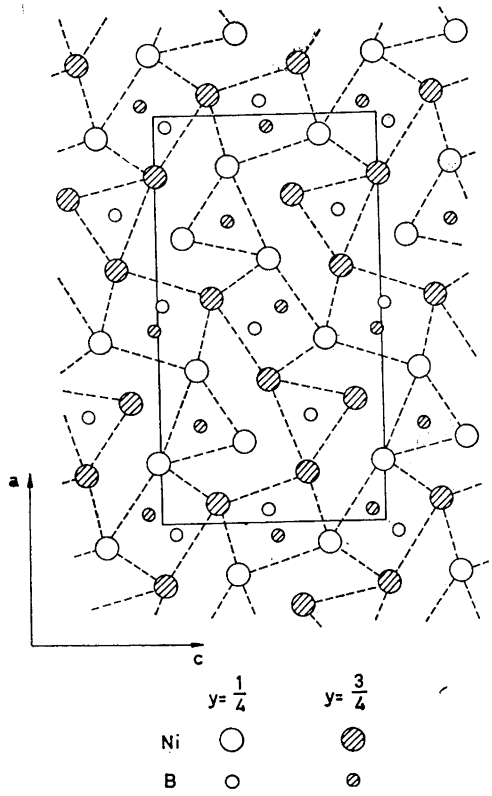

Fig. 1. The structure of orthorhombic Ni_4B_3 projected on (010).

From the crystal-chemical point of view, the *o*-Ni_4B_3 structure may thus be regarded as an intermediate between, *e.g.*, the Ni_3B (cementite type) structure [9], containing isolated boron atoms in the centers of trigonal metal atom prisms, and the FeB type structure [3] containing infinite chains of boron atoms, arranged in a way similar to *o*-Ni_4B_3. For comparison, the FeB structure (based on the same space group as *o*-Ni_4B_3) is shown in projection on the *ac*-plane in Fig. 2.

The three types of trigonal nickel atom prisms in *o*-Ni_4B_3 are shown in Fig. 3a, b and c, together with the environments of the B_I, B_{II} and B_{III} atoms. The triangular sides of the prisms are almost perpendicular to the rectangular sides; the deviations from 90° of the prisms I and II are at the limit of experimental error. The coordination number of the boron atoms is nine, the B_I and B_{II} atoms have seven nickel neighbours and two boron neighbours, and the B_{III} atoms have nine nickel neighbours.

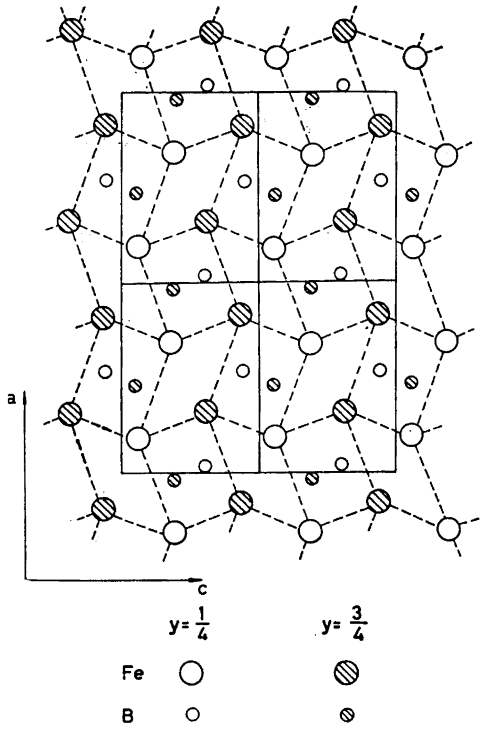

Fig. 2. The structure of FeB projected on (010).

THE STRUCTURE DETERMINATION OF MONOCLINIC Ni_4B_3

The unit cell volume of m-Ni_4B_3, 238.8 Å^3 is almost the same as that of o-Ni_4B_3, which shows that the unit cell content of m-Ni_4B_3 should be 16 nickel atoms and 12 boron atoms. The following conditions for possible reflexions were found: (h k l) only for $h + k = 2n$ and (h 0 l) only for $l = 2n$. This gives C c or $C/2c$ as possible space groups. The Patterson section $P(x$ 0 $z)$ was calculated with the threedimensional intensity material from the layer lines 0—6 around the b-axis. This section contained several large maxima, and indicated strongly that the space group is $C2/c$. Therefore, an attempt was made to interpret the Patterson section in accord with space group $C2/c$.

Large maxima were situated at the following approximate positions: (0, 0, 0) height 1; ± (0.08, 0, 0.46) height 1/4; ± (0.41, 0, 0.06) height 1/3 and (1/2, 0, 1/2) height 1/2. The maximum at ± (0.41, 0, 0.06) was unsymmetrically extended in the c direction. It was assumed that all these maxima corresponded mainly to Ni-Ni vectors. Since no maxima were found on either the a or the c axis, the positions 4(a) and 4(b) were ruled out. The 4(c) and 4(d) positions could not be occupied simultaneously, since in that case maxima at (1/2, 0, 0) and (0,0, 1/2) should exist. If the 4(e) position contained two four-fold sets of nickel atoms, the difference between their y parameters must be 1/2, because the b-axis is only 4.88 Å while the normal nickel atom radius is about 1.24 Å. The resulting maxi-

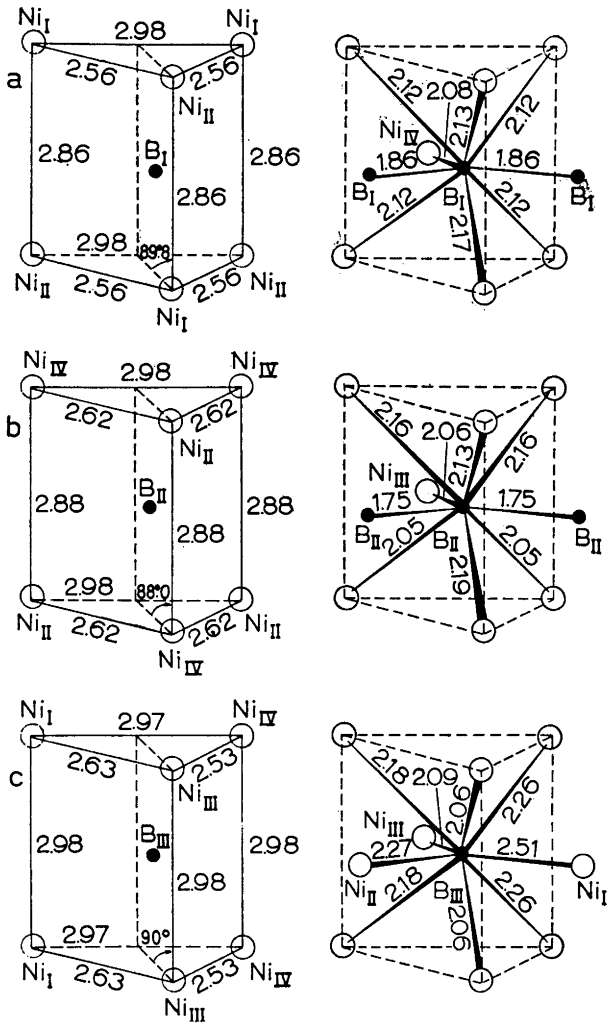

Fig. 3. The environment of the boron atoms in orthorhombic Ni_4B_3
a. the environment of the B_I atoms
b. the environment of the B_{II} atoms
c. the environment of the B_{III} atoms

mum at (0, 1/2, 0) is equivalent to a maximum at (1/2, 0, 0) and since no large maximum existed at (1/2, 0, 0), the 4(*e*) position cannot be occupied by more than four nickel atoms. The following possibilities thus remained: either sixteen nickel atoms in two 8(*f*) positions or eight nickel atoms in 8(*f*), four nickel atoms in 4(*e*) and four nickel atoms in either 4(*c*) or 4(*d*). An analysis of the last possibility did not lead to any acceptable solution, but a satisfactory explanation of the Patterson section $P(x, 0, z)$ was found by placing the nickel atoms in two 8(*f*) positions, one with $x_I = 0.04$; $z_I = 0.48$, and the other with $x_{II} = 0.20$; $z_{II} = 0.29$; this gives Harker maxima at $\pm$ (0.08, 0, 0.46) and $\pm$(0.40, 0, 0.08) with heights 1/4. If the Ni_I atoms have the y_I parameter $\pm$ 1/4, the observed maximum

Table 6. Observed and calculated $F(h0l)$- and $F(hk0)$-values for monoclinic Ni_4B_3.

h k l	F_o	F_c	h k l	F_o	F_c
0 0 0	—	508	12 0 12	—	13.0
2 0 0	—	— 8.0	0 0 14	72.0	64.9
4 0 0	146.9	137.0	2 0 14	—	—22.5
6 0 0	—	10.6	4 0 14	64.4	71.9
8 0 0	105.0	—94.0	6 0 14	—	34.6
10 0 0	—	4.0	8 0 14	—	6.8
12 0 0	101.3	—94.3	10 0 14	34.6	32.5
14 0 0	—	— 8.1	0 0 16	—	—30.9
16 0 0	—	— 9.0	2 0 16	70.6	61.5
0 0 2	25.4	23.0	4 0 16	—	6.4
2 0 2	223.2	291.7	6 0 16	45.6	50.0
4 0 2	—	—18.3	8 0 16	30.9	34.9
6 0 2	34.8	31.2	0 0 18	—	7.7
8 0 2	—	—12.0	2 0 18	—	—24.9
10 0 2	108.8	—103.8	4 0 18	54.6	58.0
12 0 2	—	— 5.6	6 0 18	—	3.9
14 0 2	73.7	—70.0	0 0 20	—	—12.2
16 0 2	—	— 7.0	2 0 20	—	22.0
0 0 4	178.0	236.5			
2 0 4	—	17.6	$\bar{2}$ 0 2	164.3	182.2
4 0 4	180.9	190.4	$\bar{4}$ 0 2	62.6	56.3
6 0 4	—	—18.8	$\bar{6}$ 0 2	122.1	—114.3
8 0 4	—	— 6.5	$\bar{8}$ 0 2	—	24.2
10 0 4	—	— 5.3	$\bar{10}$ 0 2	145.5	—142.4
12 0 4	94.9	—86.5	$\bar{12}$ 0 2	—	—13.9
14 0 4	—	7.7	$\bar{14}$ 0 2	—	—38.3
16 0 4	38.3	—46.9	$\bar{16}$ 0 2	—	—21.0
0 0 6	56.9	64.5	$\bar{2}$ 0 4	75.3	87.3
2 0 6	152.6	186.0	$\bar{4}$ 0 4	53.4	—45.7
4 0 6	33.8	—23.8	$\bar{6}$ 0 4	39.9	—46.7
6 0 6	120.7	115.5	$\bar{8}$ 0 4	147.7	—139.7
8 0 6	57.5	—49.0	$\bar{10}$ 0 4	—	—21.6
10 0 6	—	—22.6	$\bar{12}$ 0 4	58.1	—48.3
12 0 6	—	—22.1	$\bar{14}$ 0 4	—	—39.1
14 0 6	65.5	—65.5	$\bar{16}$ 0 4	—	37.7
0 0 8	26.4	30.0	$\bar{2}$ 0 6	—	— 1.8
2 0 8	71.0	78.0	$\bar{4}$ 0 6	64.0	69.3
4 0 8	131.2	129.6	$\bar{6}$ 0 6	151.6	—156.8
6 0 8	—	—10.2	$\bar{8}$ 0 6	—	—16.2
8 0 8	66.5	59.0	$\bar{10}$ 0 6	93.1	—90.0
10 0 8	—	—32.2	$\bar{12}$ 0 6	51.4	—53.2
12 0 8	—	—32.4	$\bar{14}$ 0 6	—	15.4
14 0 8	—	— 9.5	$\bar{2}$ 0 8	98.0	117.5
0 0 10	77.5	87.7	$\bar{4}$ 0 8	142.4	—129.5
2 0 10	52.0	50.8	$\bar{6}$ 0 8	—	21.6
4 0 10	—	47.5	$\bar{8}$ 0 8	100.1	—105.0
6 0 10	99.2	90.4	$\bar{10}$ 0 8	55.6	—56.4
8 0 10	—	—32.1	$\bar{12}$ 0 8	—	5.2
10 0 10	—	—31.4	$\bar{14}$ 0 8	—	—40.7
12 0 10	37.6	—35.1	$\bar{2}$ 0 10	69.4	—76.5
0 0 12	46.7	—35.2	$\bar{4}$ 0 10	—	18.2
2 0 12	78.0	89.0	$\bar{6}$ 0 10	104.5	—99.2
4 0 12	54.4	56.7	$\bar{8}$ 0 10	73.7	—78.4
6 0 12	—	20.0	$\bar{10}$ 0 10	—	—10.3
8 0 12	73.7	67.0	$\bar{12}$ 0 10	64.7	—72.0
10 0 12	—	—35.3	$\bar{2}$ 0 12	60.0	57.9

Table 6. Contd.

h k l	F_o	F_c	h k l	F_o	F_c
$\bar{4}$ 0 12	91.1	−86.0	0 4 0	81.4	88.0
$\bar{6}$ 0 12	—	−46.3	2 4 0	98.4	111.7
$\bar{8}$ 0 12	—	−29.3	4 4 0	—	29.5
$\bar{10}$ 0 12	73.2	−71.6	6 4 0	—	− 5.5
$\bar{2}$ 0 14	71.2	−70.5	8 4 0	47.8	−38.4
$\bar{4}$ 0 14	—	−33.8	10 4 0	63.1	−57.5
$\bar{6}$ 0 14	—	−39.0	1 5 0	—	8.9
$\bar{8}$ 0 14	80.6	89.0	3 5 0	39.0	−39.6
$\bar{10}$ 0 14	—	19.0	5 5 0	39.4	33.2
$\bar{2}$ 0 16	—	−14.1	7 5 0	—	−30.2
$\bar{4}$ 0 16	—	−22.6	9 5 0	—	5.3
$\bar{6}$ 0 16	72.4	−82.7	11 5 0	—	5.1
$\bar{8}$ 0 16	—	14.5	0 6 0	146.6	−168.7
$\bar{2}$ 0 18	—	−28.9	2 6 0	—	− 8.4
$\bar{4}$ 0 18	53.8	−64.8	4 6 0	69.5	−70.2
$\bar{6}$ 0 18	—	− 5.8	6 6 0	—	− 4.2
$\bar{2}$ 0 20	41.7	−47.0	8 6 0	62.9	57.4
			10 6 0	—	4.5
1 1 0	38.5	−36.6	12 6 0	63.3	64.5
3 1 0	123.2	110.0	1 7 0	—	16.7
5 1 0	100.2	−94.3	3 7 0	53.9	−53.3
7 1 0	73.0	70.4	5 7 0	48.4	55.0
9 1 0	—	−20.0	7 7 0	40.4	−46.5
11 1 0	—	− 8.2	9 7 0	—	16.1
13 1 0	—	32.3	0 8 0	—	0.2
0 2 0	43.5	−44.1	2 8 0	92.0	99.0
2 2 0	164.0	−216.0	4 8 0	—	3.5
4 2 0	—	−17.9	6 8 0	—	−13.7
6 2 0	—	18.4	8 8 0	—	3.7
8 2 0	—	13.1	10 8 0	72.2	−71.3
10 2 0	95.3	95.0	1 9 0	—	7.7
12 2 0	—	21.1	3 9 0	—	−29.8
1 3 0	—	−12.3	5 9 0	—	37.5
3 3 0	—	26.7	010 0	61.3	−58.5
5 3 0	—	29.7	210 0	—	−25.0
7 3 0	—	21.6	111 0	—	2.9
9 3 0	—	− 9.8	012 0	62.5	53.1
11 3 0	—	− 1.2			

at (1/2, 0, 1/2) is explained, and furthermore a maximum at ± (0.42, 0, 0.04), height 1/4, must exist. The large maximum observed at ± (0.41, 0, 0.06) is thus explained as resulting from an overlap of maxima at ± (0.40, 0, 0.08) and ± (0.42, 0, 0.04). From space considerations, the y_{II} parameter of the Ni_{II} atoms should have a value near 0.57, if the y_I parameter is taken to be 0.25.

The following approximate nickel positions were thus derived:

$$8\ Ni_I \text{ in } 8(f)\text{: } x_I = 0.04;\ y_I = 0.25;\ z_I = 0.48$$
$$8\ Ni_{II} \text{ in } 8(f)\text{: } x_{II} = 0.20;\ y_{II} = 0.57;\ z_{II} = 0.29$$

Signs of the $F(h\ 0\ l)$- and the $F(h\ k\ 0)$-values were computed from the model, and the electron density projections $\varrho\ (x\ z)$ and $\varrho\ (x\ y)$ were calculated, with the use of the intensity material from the zero layer lines around the b and the c axis. In addition to the nickel maxima, boron maxima corresponding to one 8(f) and one 4(e) position became visible. The two projections were refined

with successive difference syntheses. The final R-values obtained were 0.105 for the $|F(h\ 0\ l)|$-values and 0.103 for the $|F(h\ k\ 0)|$-values; an empirical temperature factor with $B = 0.20$ Å^2 was applied in both cases. The boron parameters obtained from the difference synthesis maps were not very accurate, but the following boron parameters were found: B_I in 8(f): $x_I = 0.234$; $y_I = -0.10_2$; $z_I = 0.437$ and B_{II} in 4(e): $y_{II} = -0.08_8$. From space considerations, the following B_I parameters seemed more reasonable: $x_I = 0.234$; $y_I = -0.091$; $z_I = 0.443$. These parameter values were wholly compatible with the experimental intensity data.

Observed and calculated $F(h\ 0\ l)$- and $F(h\ k\ 0)$-values are compared in Table 6.

The final structure of monoclinic Ni_4B_3 is the following:

Space group $C2/c$—(C_{2h}^6); $Z = 4$;

$a = 6.430$ Å; $b = 4.882$ Å; $c = 7.818$ Å; $\beta = 103°18'$; $U = 238.8$ Å^3; $D_x = 7.43$ g.cm^{-3}

		x	y	z
8 Ni_I	in 8(f):	0.043_5	0.250	0.483_9
8 Ni_{II}	in 8(f):	0.202_9	0.568	0.287_7
8 B_I	in 8(f):	0.23_4	0.09_1	0.44_3
8 B_{II}	in 8(e):	—	0.08_8	—

Interatomic distances are given in Table 7.

Table 7. Interatomic distances in monoclinic Ni_4B_3 (Distances shorter than 3.2 Å listed).

	Ni_I	Ni_{II}	B_I	B_{II}
Ni_I	2.53 (2), 2.61	2.52, 2.53, 2.56, 2.63 2.79, 2.81, 3.15	2.0_9, 2.1_3 2.1_4, 2.1_8	2.3_0 2.4_3
Ni_{II}	2.52, 2.53, 2.56, 2.63 2.79, 2.81, 3.15	2.62 (2), 2.54	2.0_4, 2.0_5 2.0_9	2.1_1 2.1_4
B_I	2.0_9, 2.1_3 2.1_4, 2.1_8	2.0_4, 2.0_5 2.0_9	1.8_3	1.8_7
B_{II}	2.3_0 (2) 2.4_3 (2)	2.1_1 (2) 2.1_4 (2)	1.8_7 (2)	

DESCRIPTION OF THE MONOCLINIC Ni_4B_3 STRUCTURE.

The m-Ni_4B_3 structure can be described as built-up by rather close-packed, slightly corrugated nickel atom layers with chains of boron atoms running through the channels in the metal atom lattice. The nickel atom layers are parallel with {202}, and the arrangement of the nickel atoms in one layer is shown schematically in Fig. 4. The {202} layers in m-Ni_4B_3 are closely related to the slightly corrugated {10$\bar{1}$1} layers in hexagonal close-packed structures, and are intermediates between the {103} layers in Ni_3B ($D\ O_{11}$ structure) and the {0 0 1} layers in Ni_2B (C 16 structure). (Compare Fig. 4 in the present paper

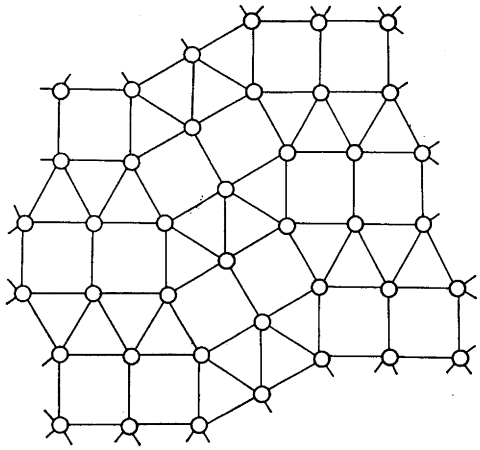

Fig. 4. Nickel atom layers parallel with {202} in monoclinic Ni_4B_3.

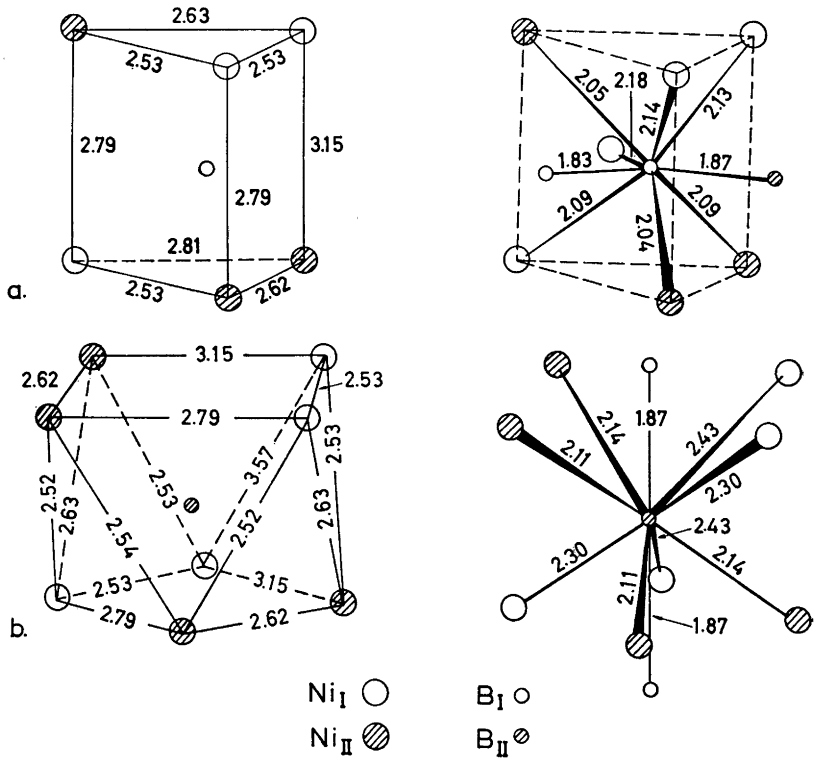

Fig. 5. The environment of the boron atoms in monoclinic Ni_4B_3
a. the environment of the B_I atoms
b. the environment of the B_{II} atoms

with Figs. 1, 2 and 3 in Ref.[9]). In Ni_3B, the boron atoms are situated in trigonal prismatic holes without forming any close B-B contacts. In Ni_2B, the boron atoms are situated in antiprismatic holes and form strings throughout the structure with a B-B distance of 2.12 Å. In *m*-Ni_4B_3, both types of holes exist; the B_I atoms occupy distorted trigonal prismatic holes, while the B_{II} atoms occupy distorted antiprismatic holes. The B_I environment is shown in Fig. 5a and the B_{II} environment in Fig. 5b. All of the boron atoms are connected in infinite chains, the sequence of which is $--B_{II}-B_I-B_I-B_{II}-B_I-B_I--$ with the B_I-B_{II} distance 1.8_7 Å and the B_I-B_I distance 1.8_3 Å. The mean Ni-B_{II} distance in the *m*-Ni_4B_3 antiprisms is 2.25 Å as compared with the Ni-B distance of 2.14 Å in the Ni_2B antiprisms.

GENERAL REMARKS

From the crystal-chemical point of view, the series of nickel borides Ni_3B, Ni_2B, *o*-Ni_4B_3, *m*-Ni_4B_3 and NiB provides a striking example of the gradually increasing B-B bond formation with increasing boron content in transition metal borides [15]. The structural similarities between the 'complicated carbides' and the nickel borides may also be noted; Ni_3B and Fe_3C are isostructural [9], while *o*-Ni_4B_3 and NiB are structurally related to Cr_3C_2 [16].

The present phase analysis has shown that the old equilibrium diagram given by Giebelshausen [1] is not reliable. The investigation of Hoppin III [2] provides accurate thermal data only up to 17 atom-% boron. It is desirable that the remaining part of the equilibrium diagram be investigated with modern metallographic and thermal analytical methods.

Acknowledgements. The author has performed this investigation during the tenure of a generous scholarship from the *Statens Tekniska Forskningsråd.* The work has been financially supported in part by the *Air Force Office of Scientific Research of the Air Research and Development Command, United States Air Force,* through its European Office under Contract No. AF 61(052)-40.

The author wishes to thank Professor G. Hägg for his kind interest. Thanks are also due Dr. B. Aronsson for many stimulating discussions.

REFERENCES

1. Giebelshausen, H. *Z. anorg. Chem.* **91** (1915) 257.
2. Hoppin III, G. S. *Welding J.* **36** (1957) 528.
3. Bjurström, T. *Arkiv Kemi, Mineral. Geol.* **11 A** (1933) No. 5.
4. Andersson, L.-H. and Kiessling, R. *Acta Chem. Scand.* **4** (1950) 160.
5. Blum, P. *J. phys. radium* **13** (1952) 430.
6. Kiessling, R. *Acta Chem. Scand.* **3** (1949) 595.
7. Marion, S. *Bull. soc. chim. France* **1957** 522.
8. Rundqvist, S. *Nature* **181** (1958) 259.
9. Rundqvist, S. *Acta Chem. Scand.* **12** (1958) 658.
10. Fruchart, R. and Michel, A. *Bull. soc. chim. France* **1958** 278.
11. Blok, N. J., Kozlova, M. N., Lashko, N. F. and Shpunt, K. Ya. *Doklady Akad. Nauk SSSR* **113** (1957) 811.
12. Rundqvist, S. and Jellinek, F. *Acta Chem. Scand.* **13** (1959) 425.
13. Thomas, L. H. and Umeda, K. *J. Chem. Phys.* **26** (1957) 293.
14. Ibers, J. A. *Acta Cryst.* **10** (1957) 86.
15. Kiessling, R. *Acta Chem. Scand.* **4** (1950) 209.
16. Hellbom, K. and Westgren, A. *Svensk Kem. Tidskr.* **45** (1933) 141.

Received March 25, 1959.